

SANS and TEM investigation of phase precipitation in HT-9 at high neutron irradiation dose levels

J. Van den Bosch, O. Anderoglu, S.A. Maloy

Los Alamos National Laboratory

Funded by DOE office of NE

Acknowledgements

- Hot cell work: T. Romero
- SANS: P. Hosemann, M. Hartl, R.P. Hjelm
- FIB: P. Dickerson
- TEM: R. Dickerson, D. Bhattacharyya
- FCRD Project management & mentor: S. Maloy

Outline

- **Introduction**

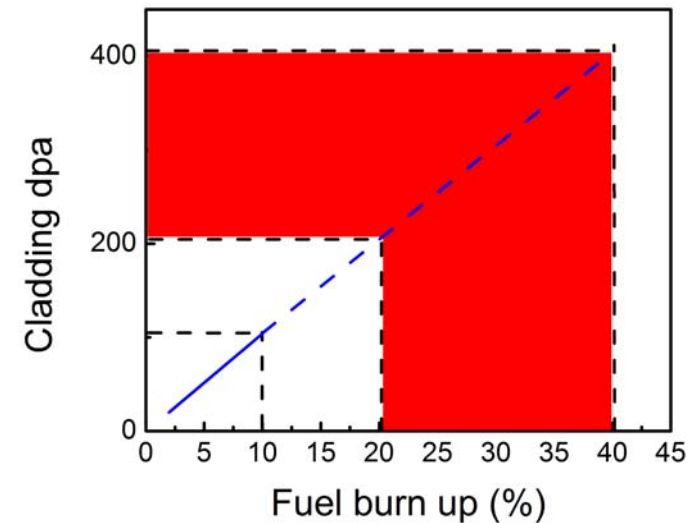
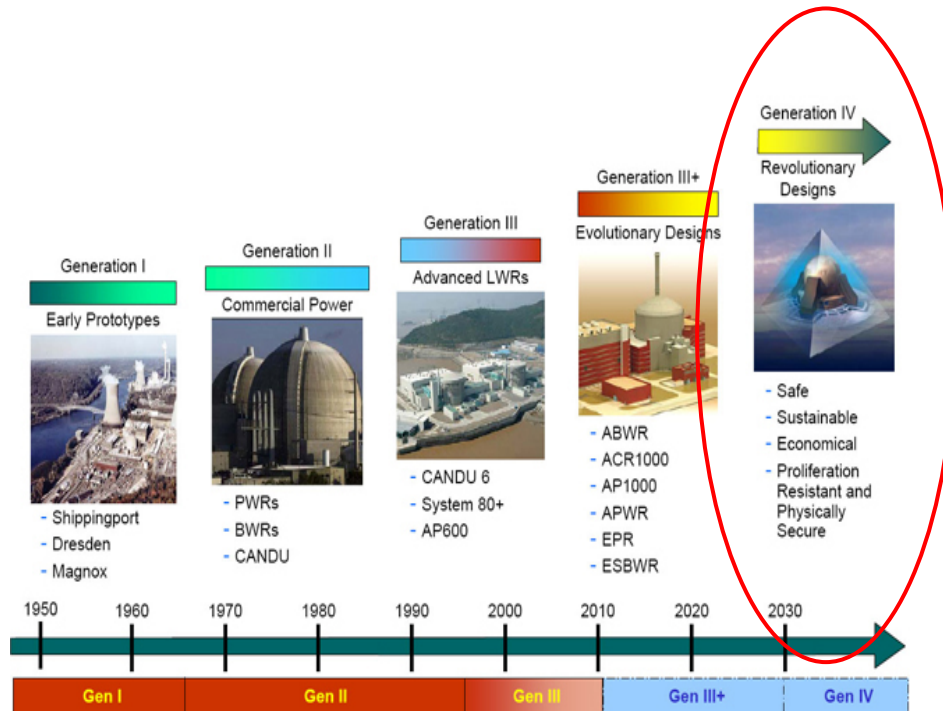
- Background and motivation
- ACO-3 duct

- **SANS & TEM analysis of the ACO-3 duct**

- SANS measurements at LANL's Lujan Center
- SANS and TEM results

- **Summary**

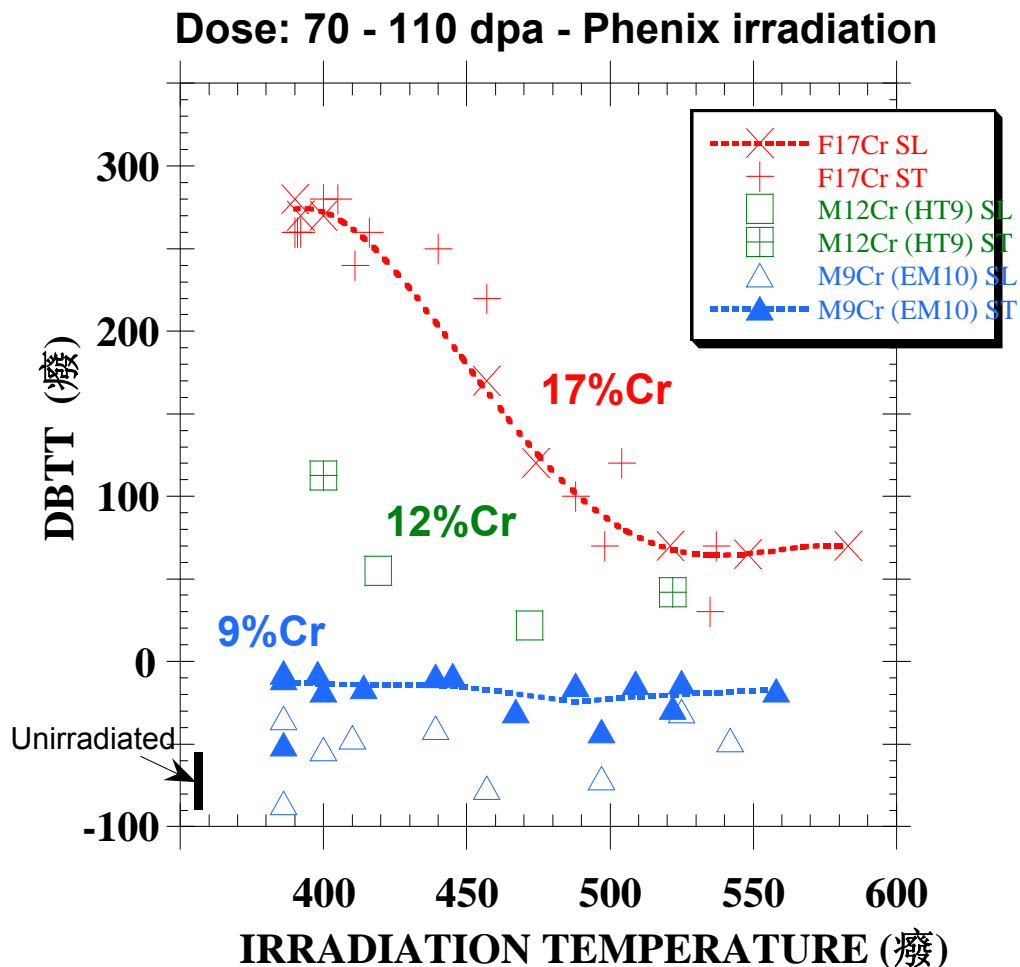
Gen IV reactors demand materials resistant to irradiation



FCRD program's objective

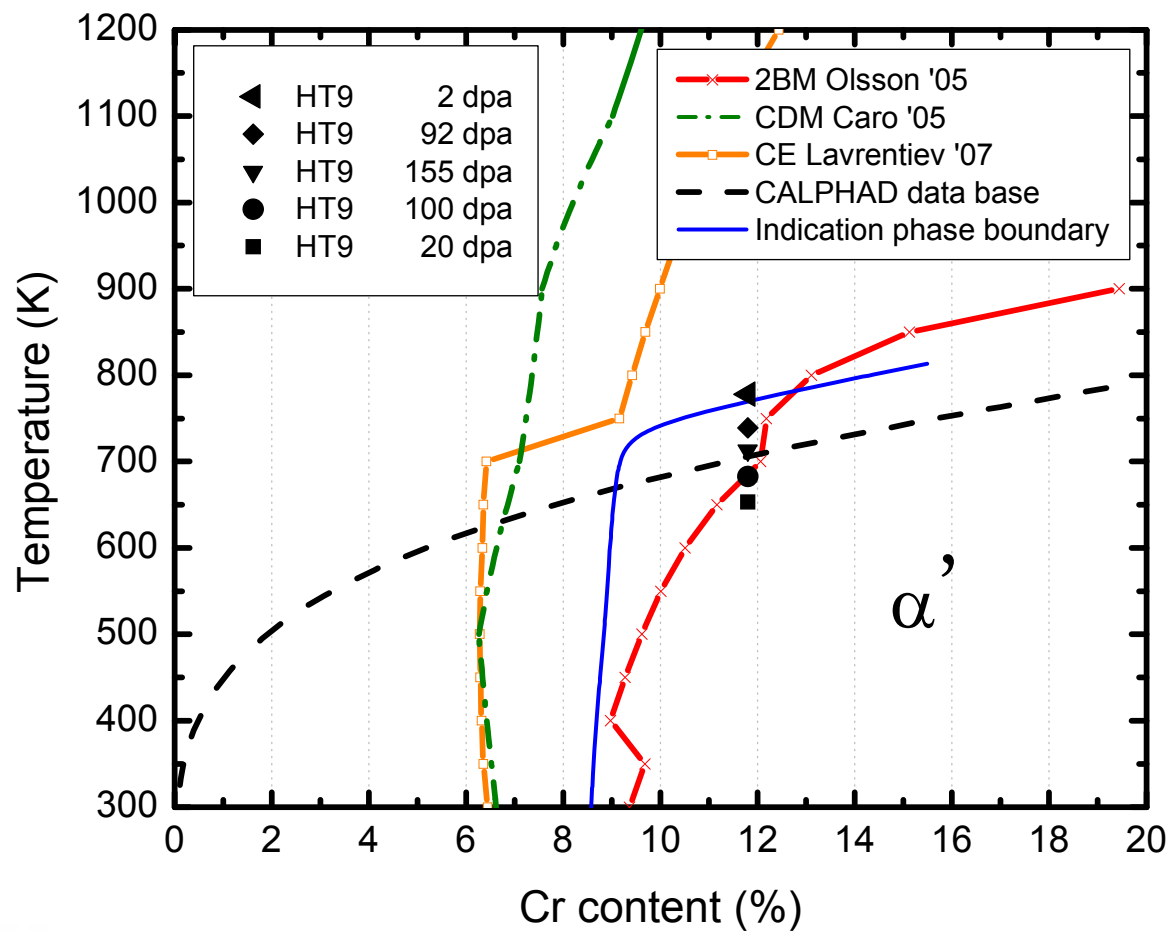
<http://www.ne.doe.gov/geniv>

Increase in Cr content suggests an increase in Ductile to Brittle Transition Temperature (DBTT)



J. L. Séran *et al.*, JNM 94

Theoretical calculations on the formation of α'

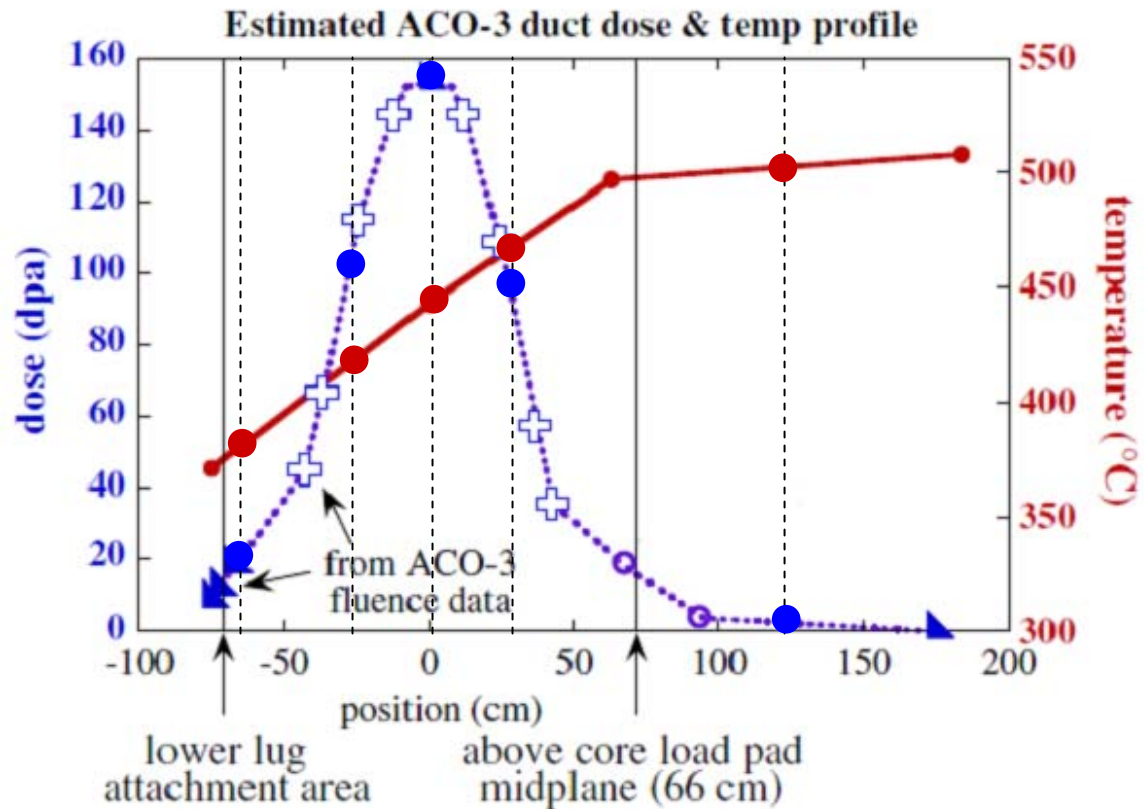
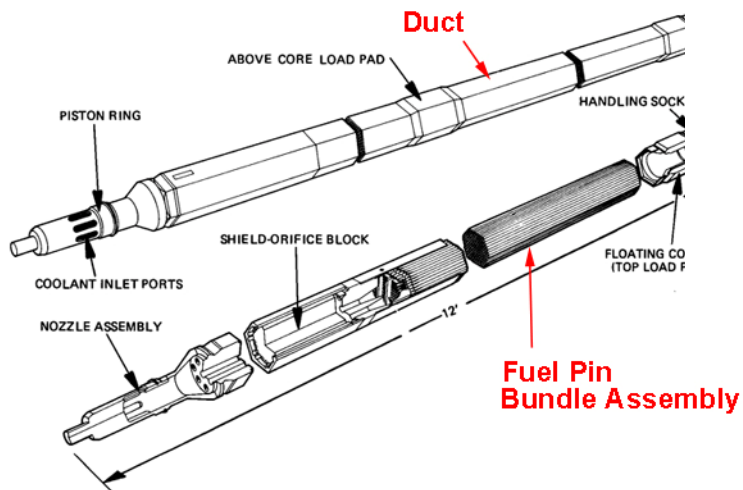


G. Bonny *et al.*, Scripta. Mat. (2008)

ACO-3 duct



FFTF, Hanford site, WA



H. Sencer *et al.* JNM (2009)

UNCLASSIFIED

Slide 7

Phases expected to form in HT-9

	Before irradiation			After irradiation							
	Precipitate	Density (m ⁻³)	Avg. Dia. (nm)	Precipitate	References						
HT-9 heat 84425	M ₂₃ C ₆ MC	7.1 × 10 ¹⁹ 1.6 × 10 ¹⁸	155 50	α' G M ₆ C (η) χ Laves MC M ₂₃ C ₆ Cavity/bubble	Kai et al JNM 96; Mathon et al JNM 03 Gelles JNM 96; Sencer et al JNM 09 Dubuisson et al JNM 93 Gelles JNM 96; Kai et al JNM 96 Gelles JNM 96 Kai et al JNM 96						
	C	N	Cr	Mo	Mn	Si	Ni	V	Nb	W	Ta
HT-9 Heat 84425	0.21	-	11.8	1.03	0.50	0.21	0.51	0.33	-	0.52	-

Structural and compositional details of phases expected to form in neutron irradiated HT-9

- α' : Local enrichment of Cr (BCC), coherent with the bcc Fe matrix.
- **G**: Has the ideal stoichiometric composition of $\text{Ti}_6\text{Ni}_{16}\text{Si}_7$. Many variations are possible: Ti is replaced by Mn, V, Nb, Ta, Zr, Hf, or **Cr**. In some cases, **Fe** and Mo substitution for Ni has been observed; e.g. $\text{Mn}_7\text{Ni}_{16}\text{Si}_7$
- χ : Chi phase, is a bcc structured Fe-Cr phase enriched in Cr and Mo compared to the matrix: e.g. $\text{Fe}_{36}\text{Cr}_{12}\text{Mo}_{10}$
- **Laves**: Laves phase has the composition AB_2 and has a cubic or hexagonal structure. In T91 or HT9, it mostly comprises of Fe_2Mo formed under irradiation at high temperature ($>500^\circ \text{C}$).
- **M_6C (η or Eta phase)**: The M_6C (η) phase is a carbide with a diamond-cubic (E9, Fd3m) structure.

Outline

- Introduction

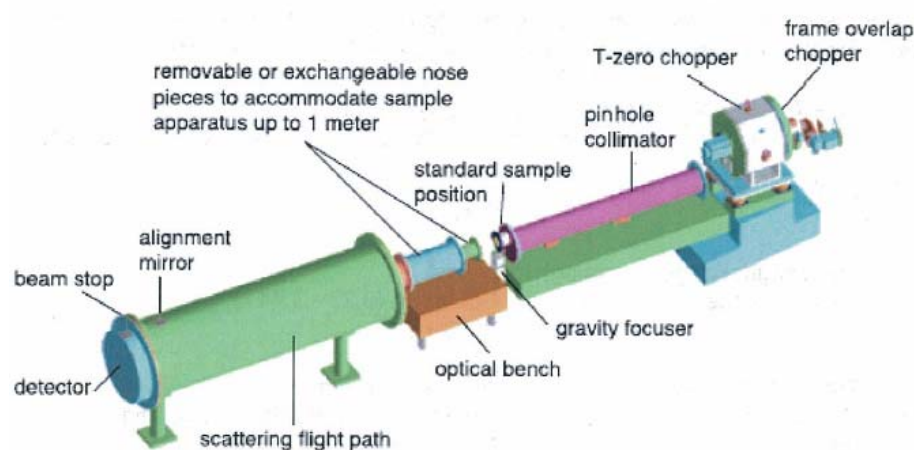
- Background
- Objective
- ACO-3 duct

- **SANS & TEM analysis of the ACO-3 duct**

- SANS measurements at LANL's Lujan Center
- SANS and TEM results

- Summary

SANS at LANL's Lujan Center



- Q range: 0.003 to 0.5 \AA^{-1}
- Source to sample: 8.40 m
- Sample to detector: 4.32 m
- Intense source of long wavelength ("cold") neutrons; $\lambda=1\text{-}16 \text{ \AA}$
- Energy and wavelength vary as TOF
- $\sim 1 \text{ nm} - 100 \text{ nm}$ features

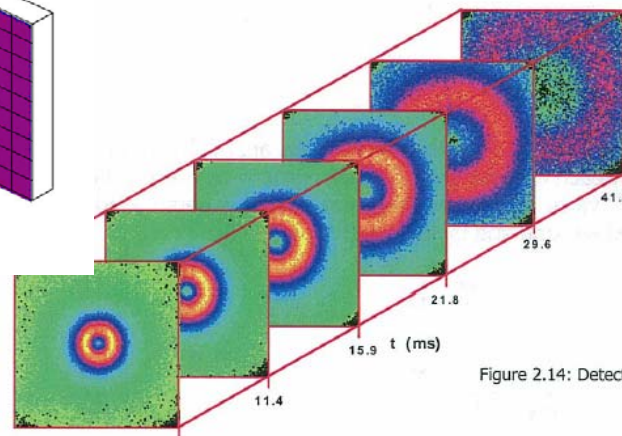
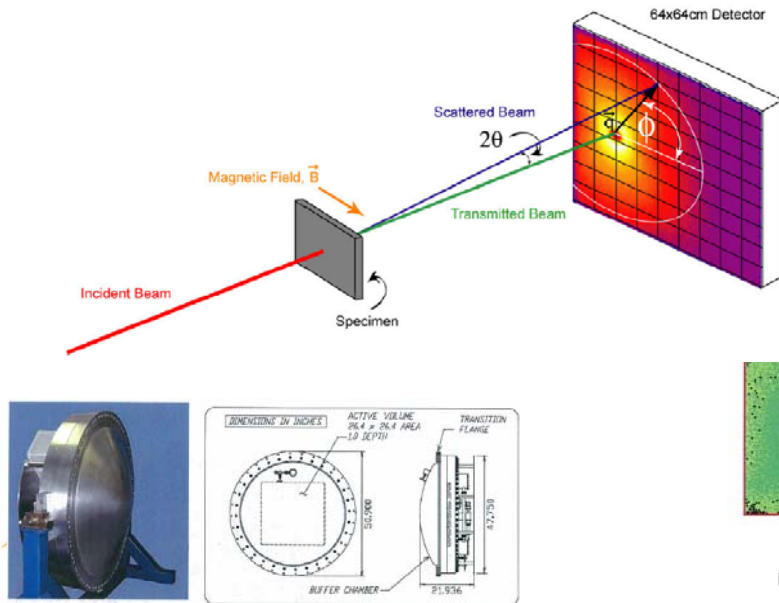
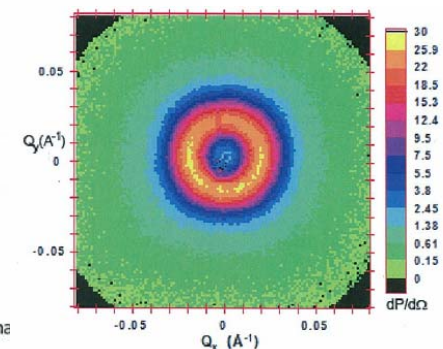


Figure 2.14: Detector maps

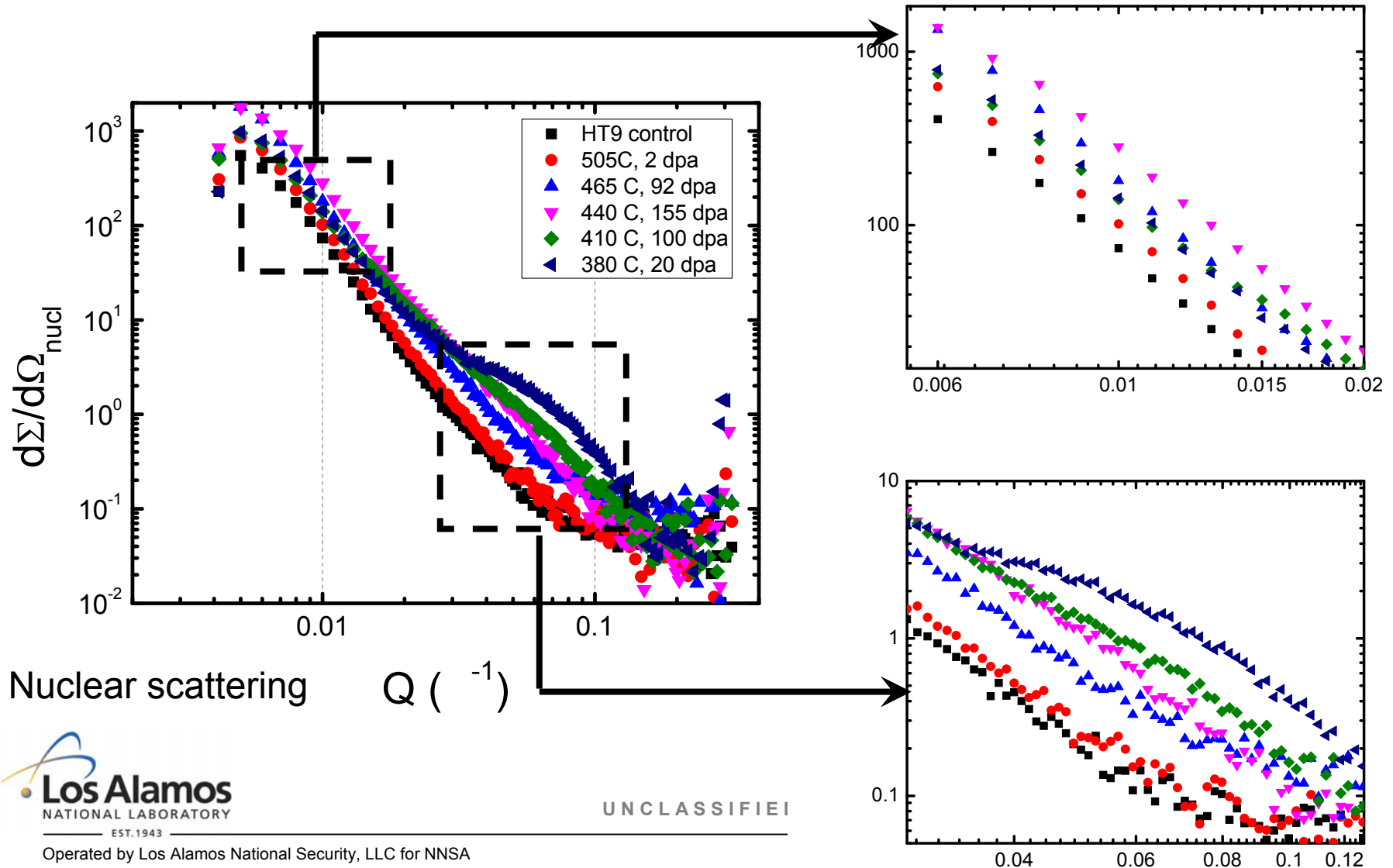


Visit: <http://www.ncnr.nist.gov/programs/sans>

UNCLASSIFIED

Slide 11

SANS analysis of the ACO-3 duct indicates formation of precipitates increases with decreasing temperature



A-ratio calculation and selected values of phases

A-ratio: the ratio between scattered intensities perpendicular and parallel to the sample magnetization.

For chemically and magnetically homogeneous particles, it is then given by: (assuming form factor $P(Q)$ is the same for nuclear and magnetic contributions)

$$A = \left(\frac{d\Sigma}{d\Omega} \right)_{\perp \vec{H}} / \left(\frac{d\Sigma}{d\Omega} \right)_{// \vec{H}} = 1 + \left(\frac{\Delta \rho_{\text{mag}}}{\Delta \rho_{\text{nuc}}}} \right)^2$$

Examples:

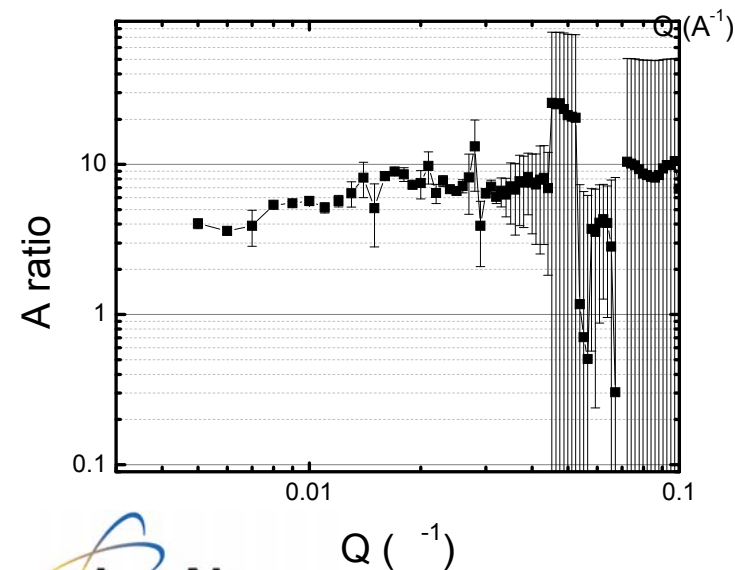
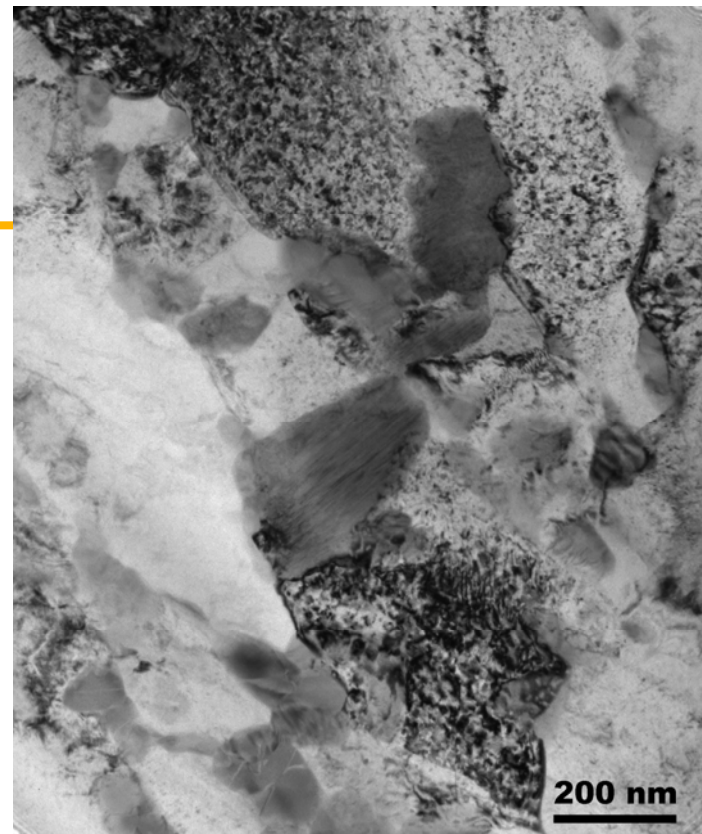
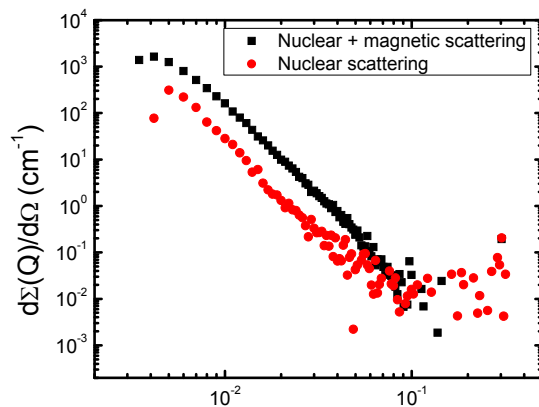
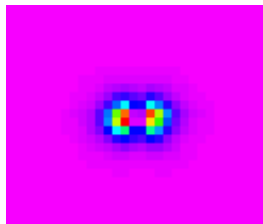
- $M_{23}C_6$ ($Cr_{0.65}Fe_{0.35}$): 3.5
- Vacancy clusters or voids: 1.0-1.4
- α' Cr precipitates: 2.03-2.13

(taking into account the average magnetic moment: $\mu=2.20$ - 2.39 C_{Cr})

- Cr-13Mo-8Fe-3Si: 2.35

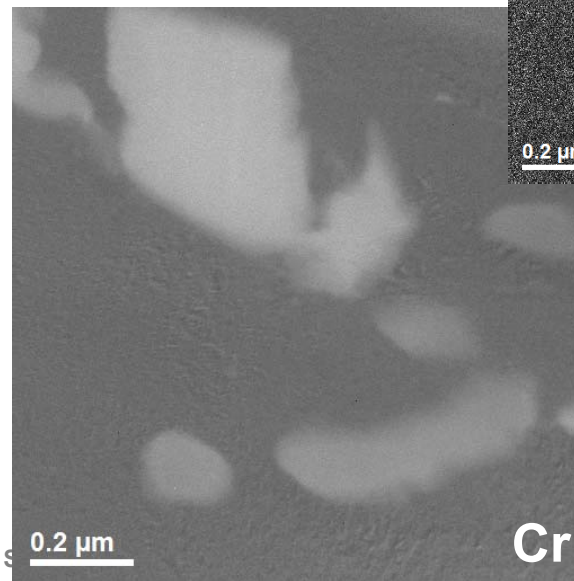
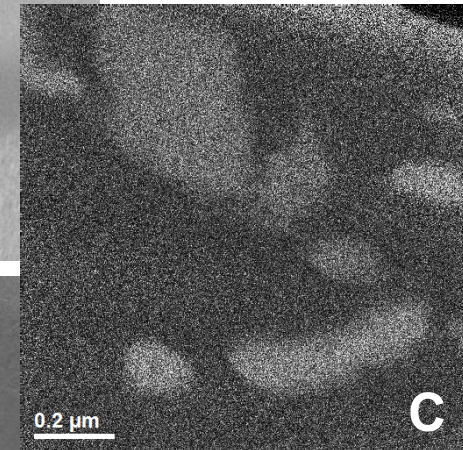
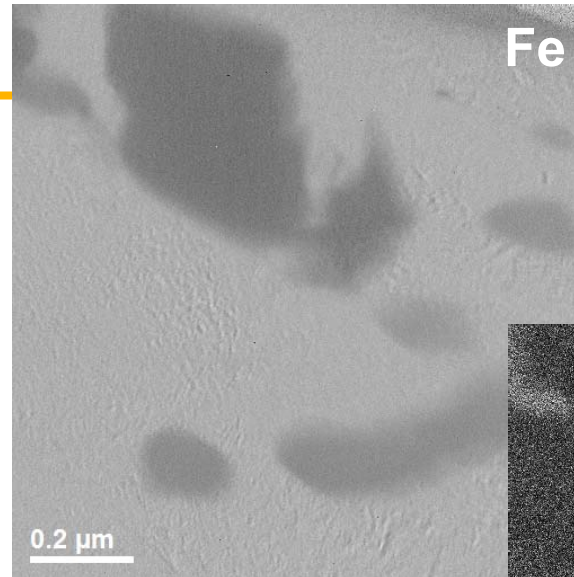
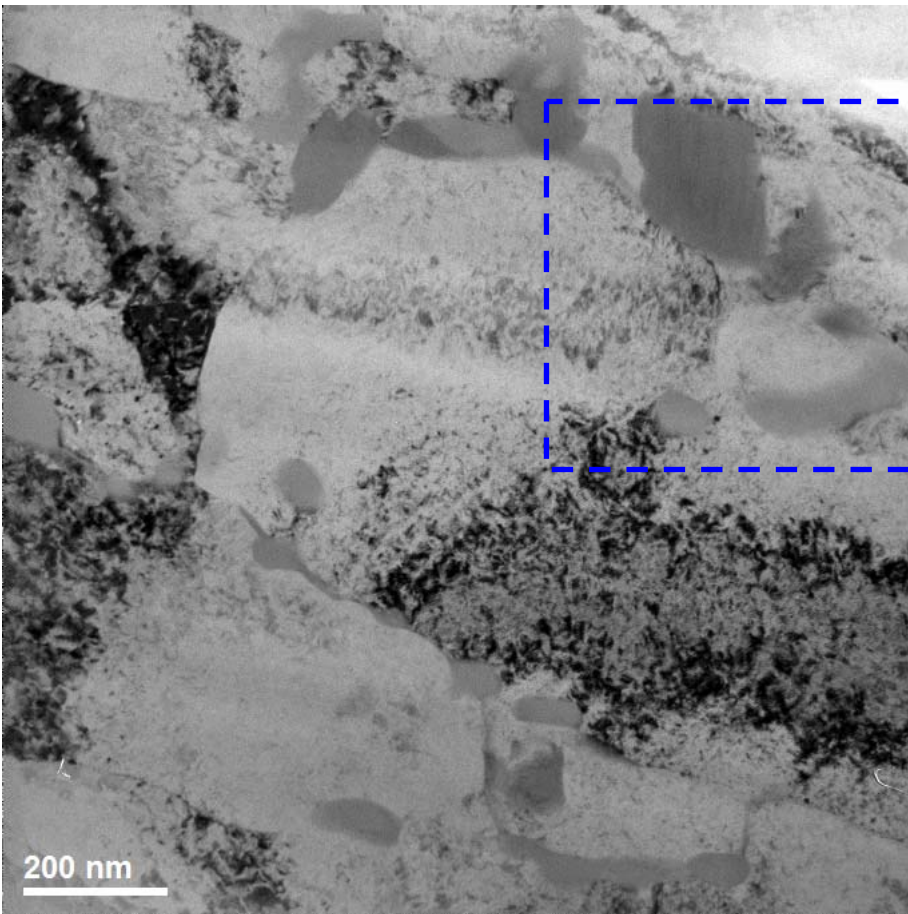
(measured by Gelles and Thomas in HT9 following neutron irradiation at 425° C to high dose)

2 dpa, 505° C zone

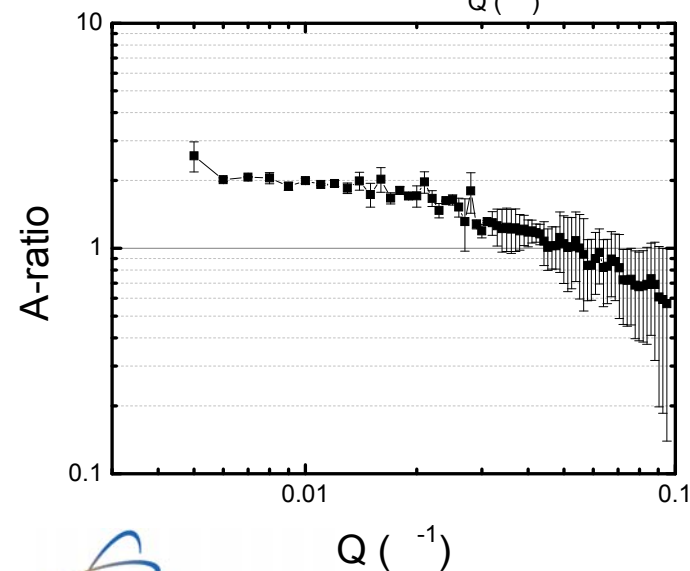
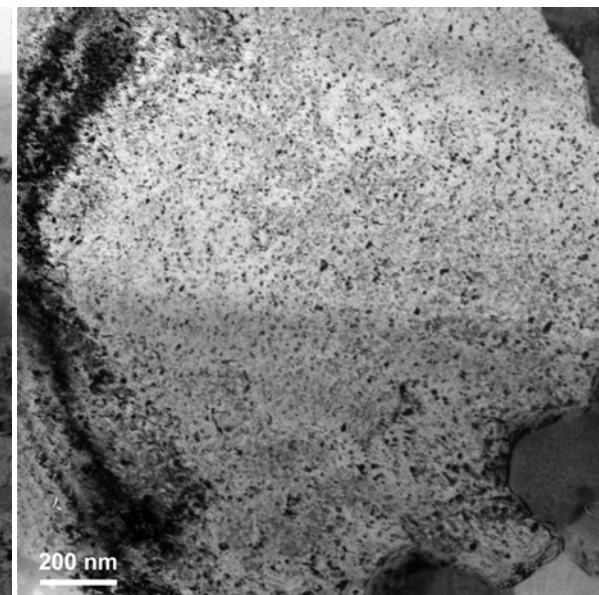
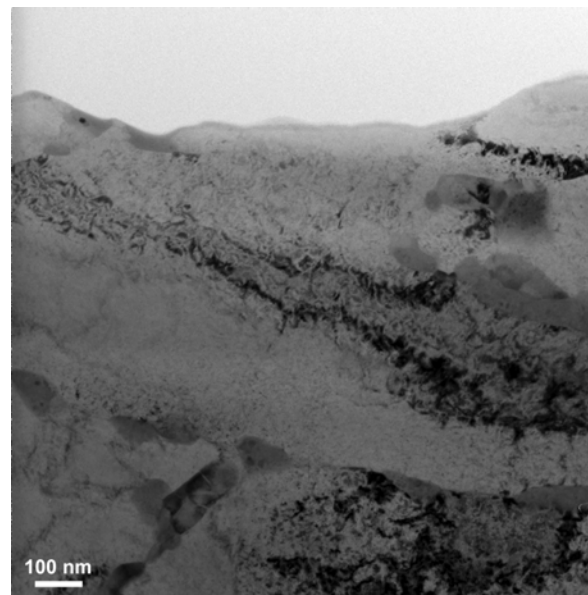
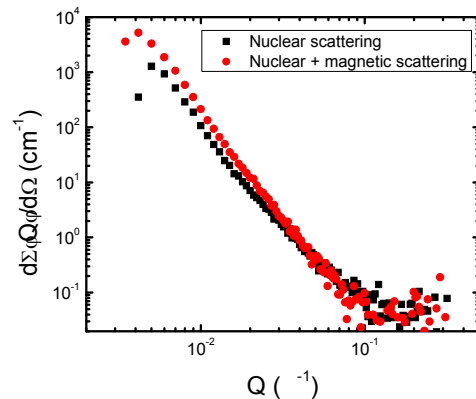
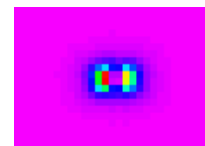


- No voids or radiation induced second phase particles observed in TEM;
- $M_{23}C_6$ decorating grain and lath boundaries;
- SANS confirmation of negligible scattering after subtraction of reference sample;
- A-ratio ~ 3 at low Q indicates carbide coarsening.

2 dpa, 505° C zone: EFTEM images



92 dpa, 466° C zone

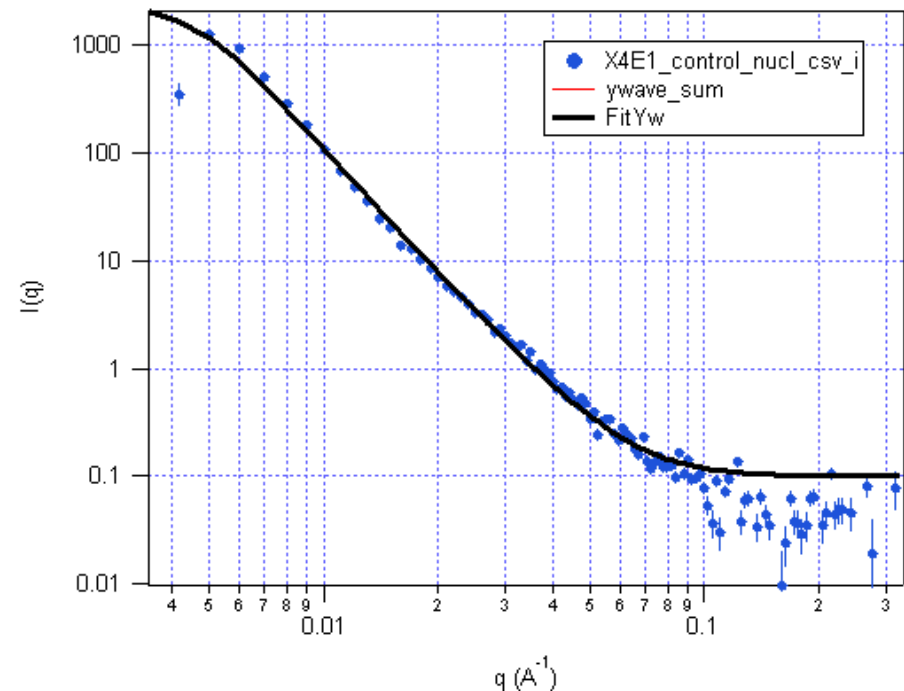


- No voids observed;
- $M_{23}C_6$ decorating grain and lath boundaries;
- Dislocations/high density of interstitial loops
- A-ratio suggests dominant presence of Cr-rich precipitates.

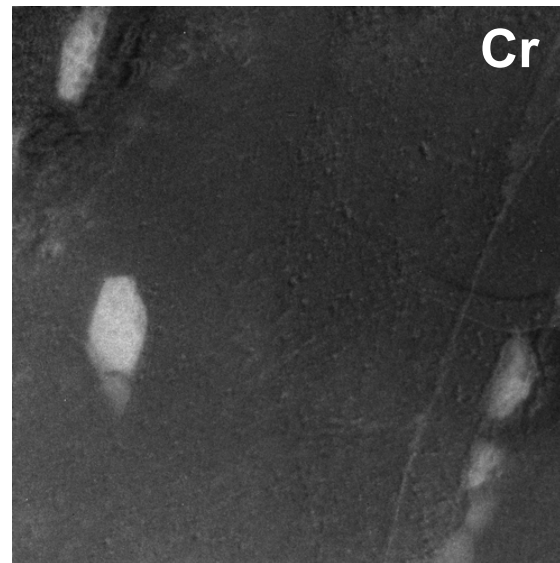
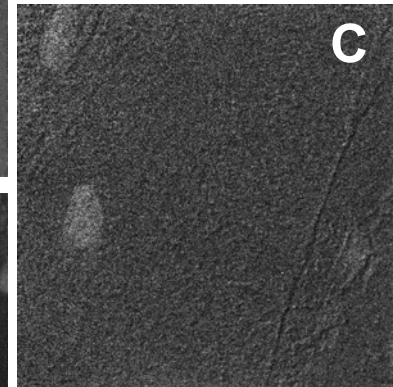
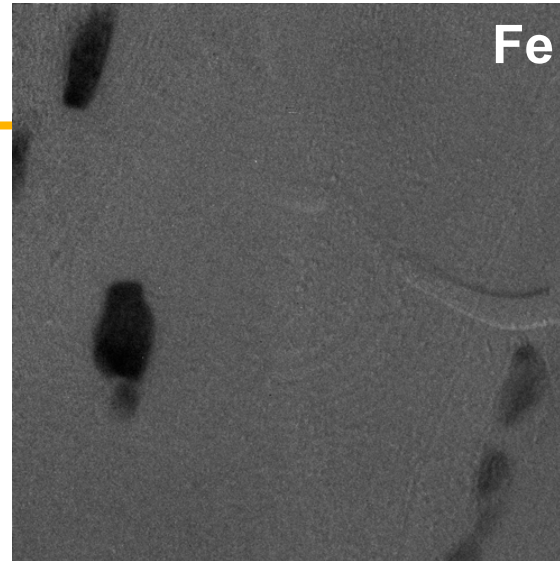
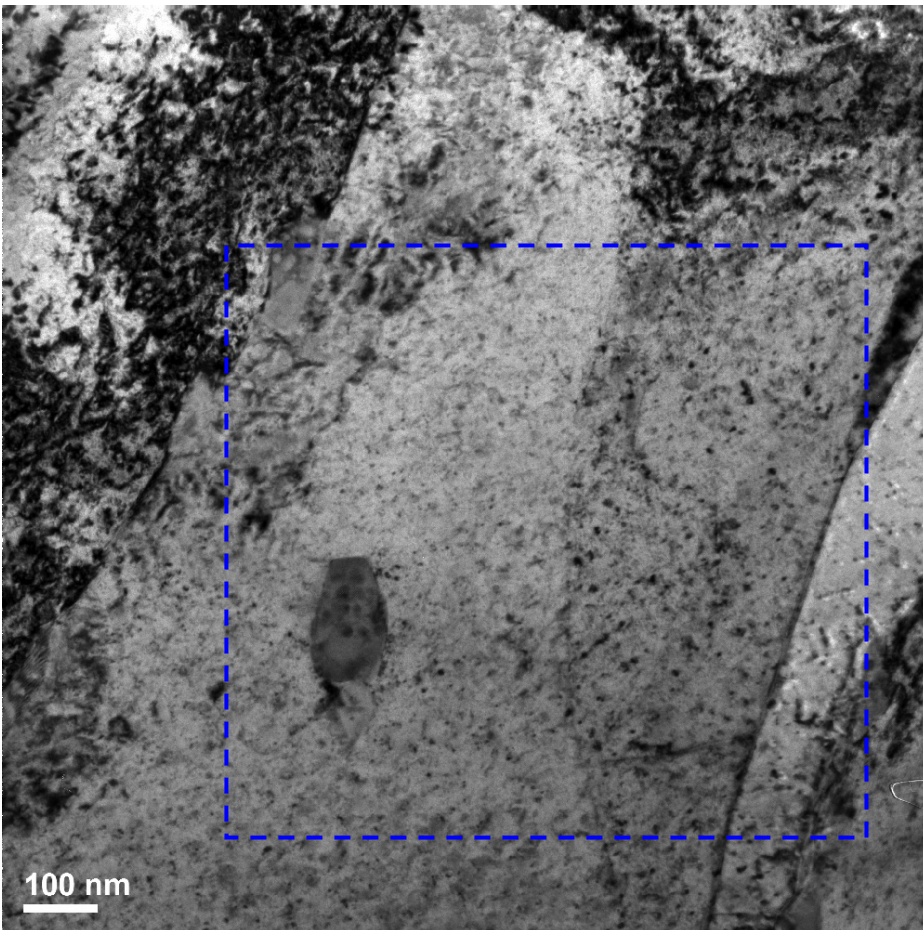
92 dpa, 466° C zone

Guinier-Porod fit of both nuclear scattering and magnetic scattering indicates:

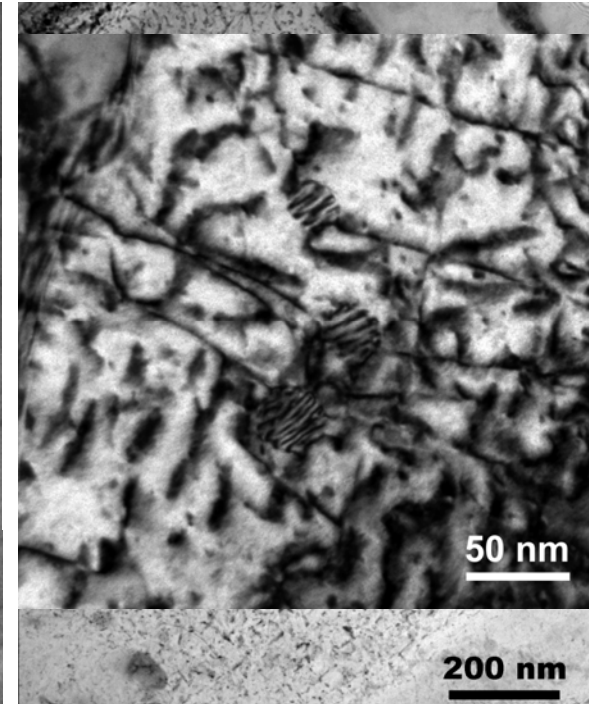
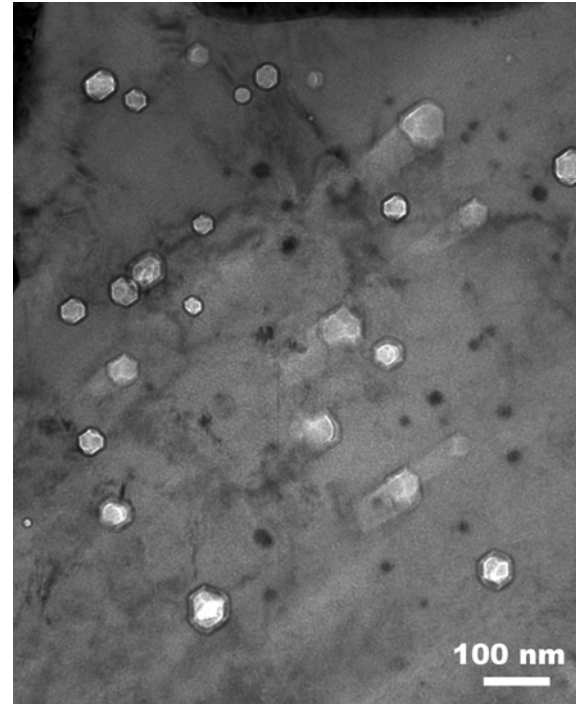
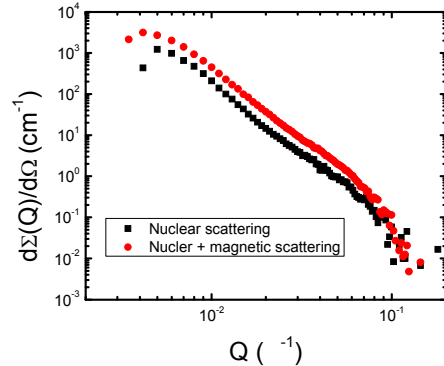
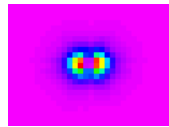
- Bimodal particle distribution
- Very small contribution of small smooth hard spheres
- Larger irregular spheroid particles
- Larger particles of ~ 90 nm dia.
- Small particles/defects of ~ 11 nm dia.



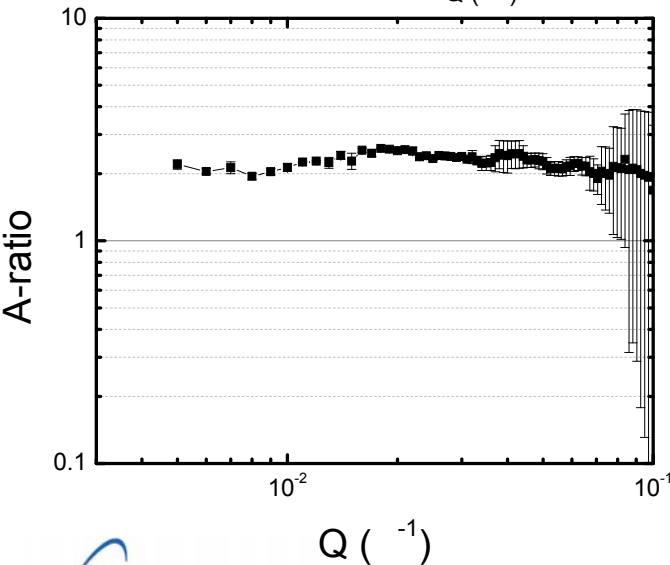
92 dpa, 466° C zone: EFTEM images



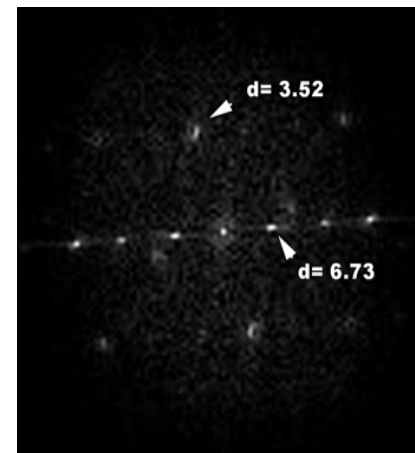
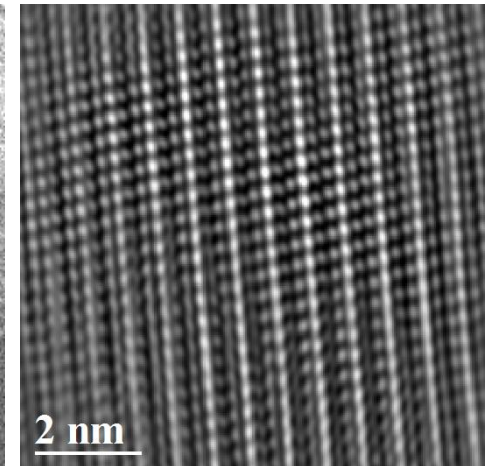
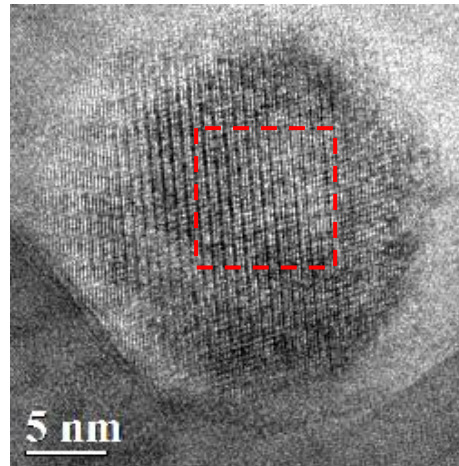
155 dpa, 440° C zone



- Average void size 42 nm, ~0.3% swelling;
- Not yet in steady state swelling regime
- G-phase found in grains (see next slide);
- A-ratio indicates Cr-rich precipitates dominant



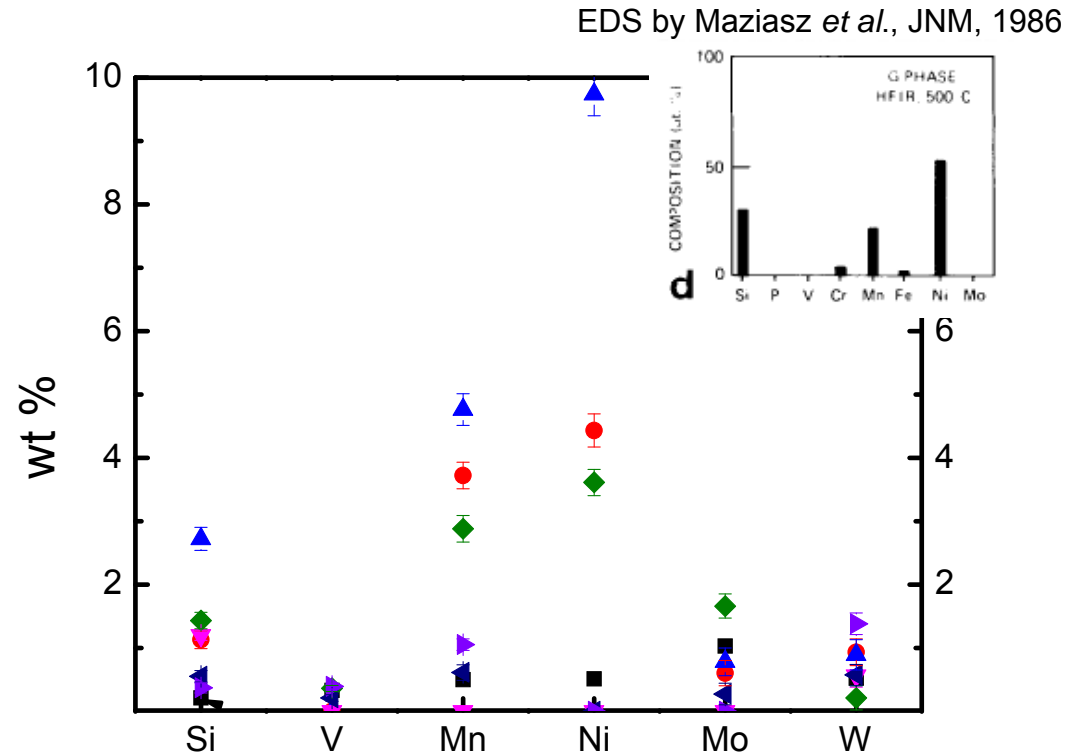
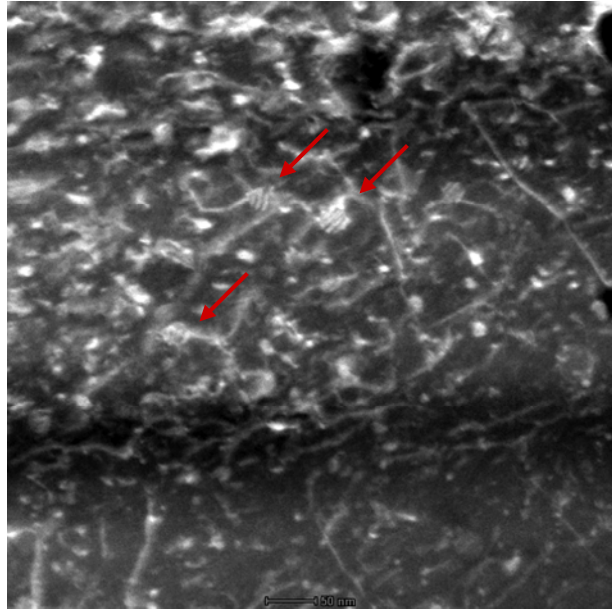
155 dpa, 440° C zone: G-phase particles



G-phase ($\text{Mn}_6\text{Ni}_{16}\text{Si}_7$): $d_{111} = 6.45$ Å; $d_{311} = 3.37$ Å

Ref. Yan *et al.*, JAC (2009) 152-155.

155 dpa, 440° C zone: G-phase particles

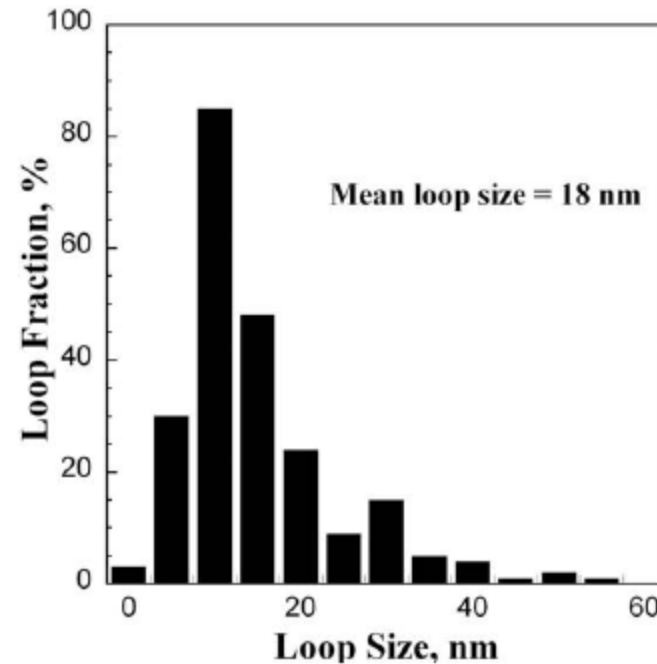
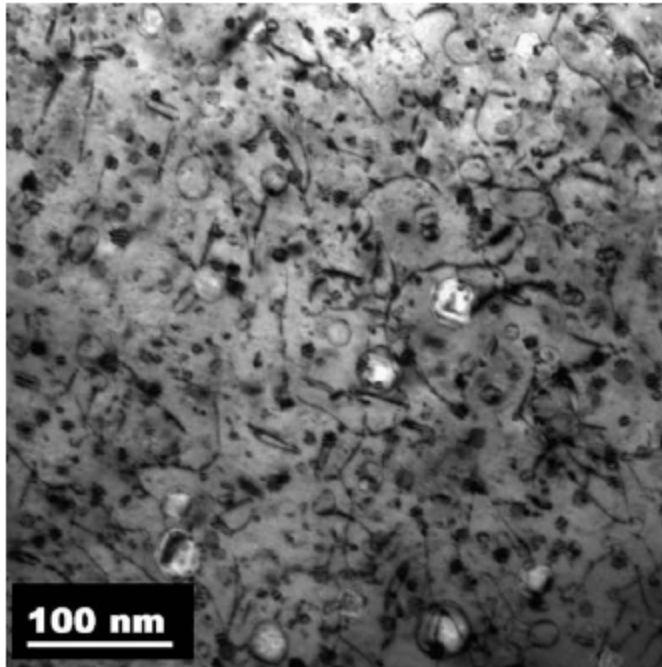


Yan *et al.*, J. Alloys and Compounds 469 (2009) 152–155: Mn₆Ni₁₆Si₇

Gelles, Thomas, FR conference (1983): Ni-24.1Fe-12.7Si-8.7Mn-3.8Mo-1.9Cr.

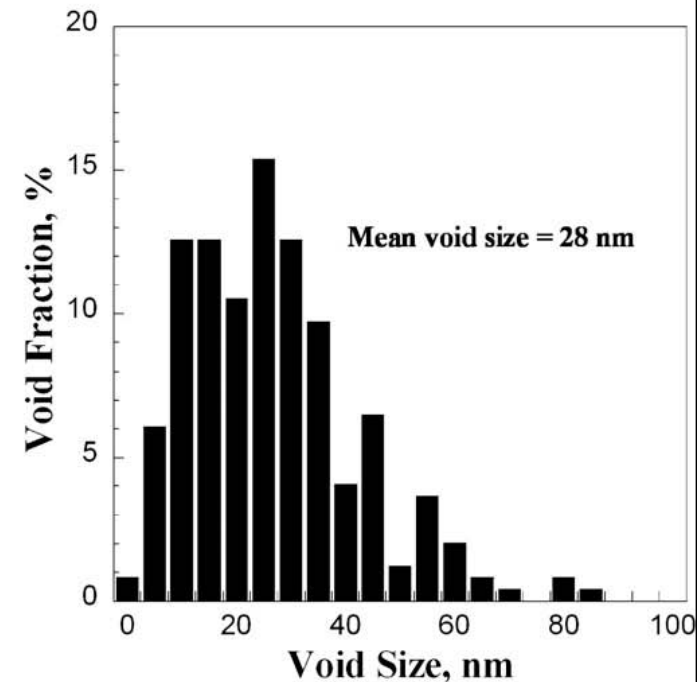
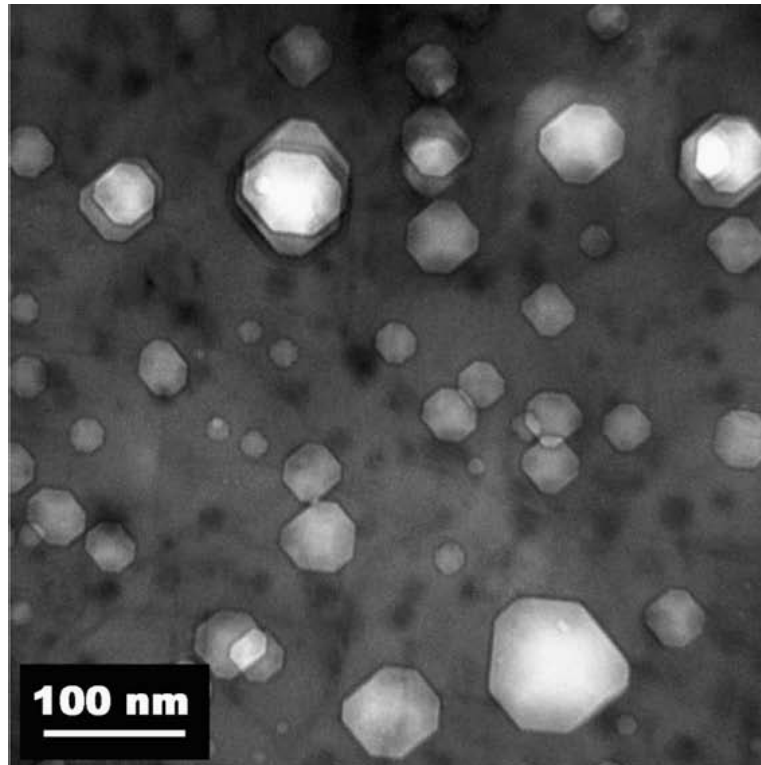
Klueh and Harries (2001): Mn₇Ni₁₆Si₁₇

155 dpa, 440°C zone: dislocations



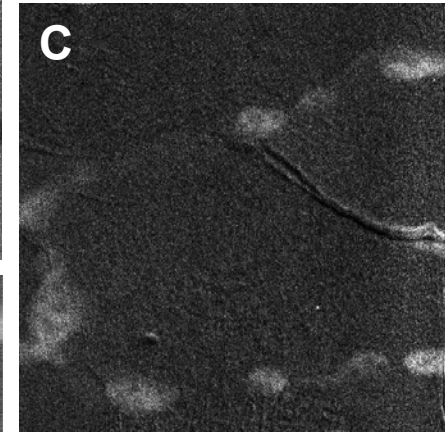
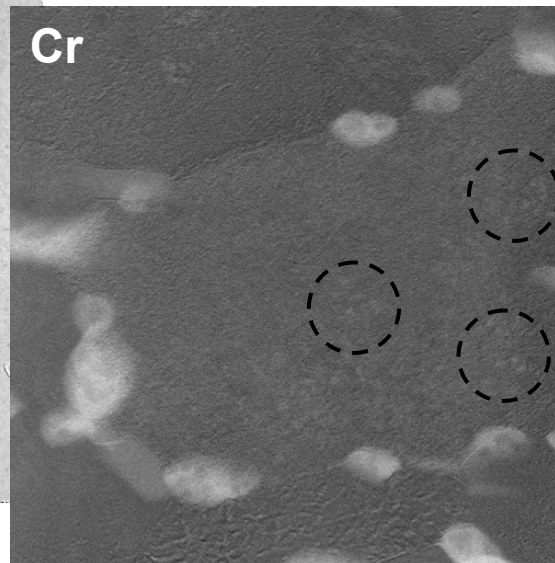
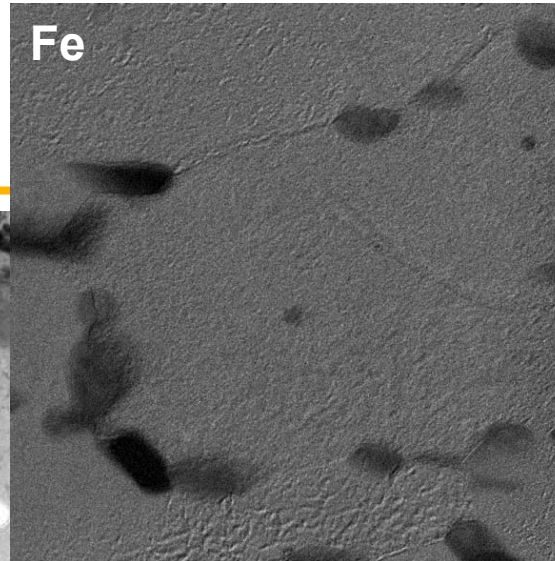
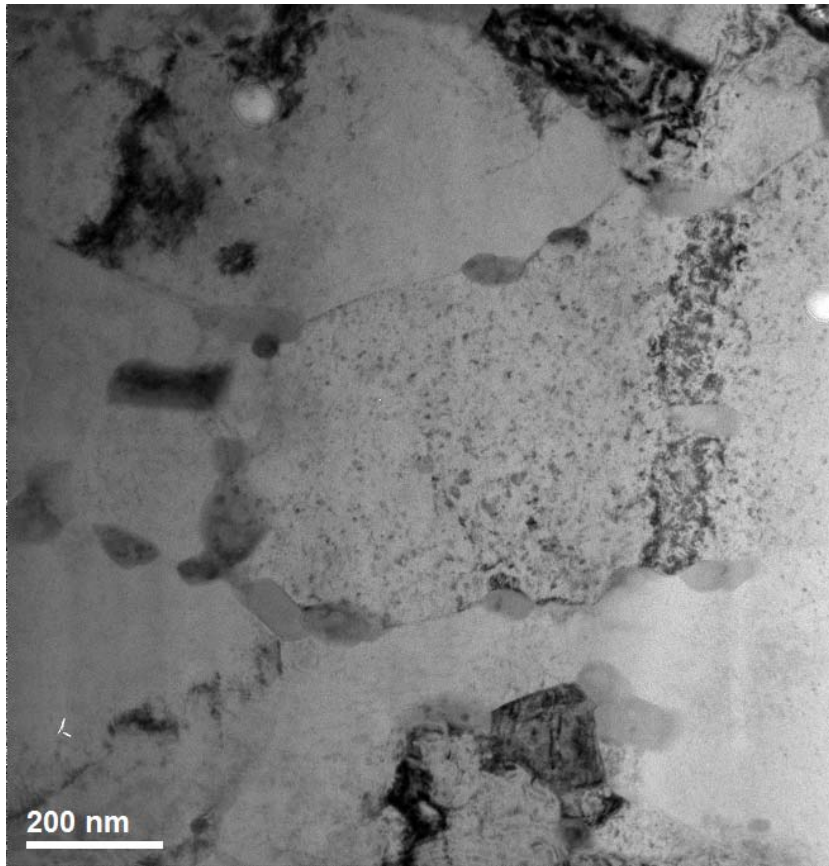
- Total network dislocation density ($(a/2)\langle 111 \rangle + a\langle 100 \rangle$): $3 \times 10^{15} \text{ m}^{-2}$
- $(a/2)\langle 111 \rangle$ dislocation (dominant) density: $2.2 \times 10^{15} \text{ m}^{-2}$.
- Loops predominantly $a\langle 100 \rangle$ type, density: $5 \times 10^{20} \text{ m}^{-3}$.

155 dpa, 440°C zone: voids



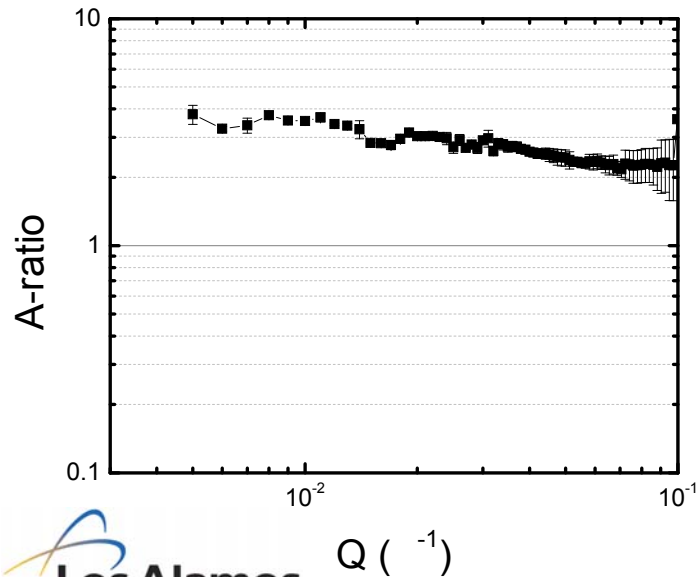
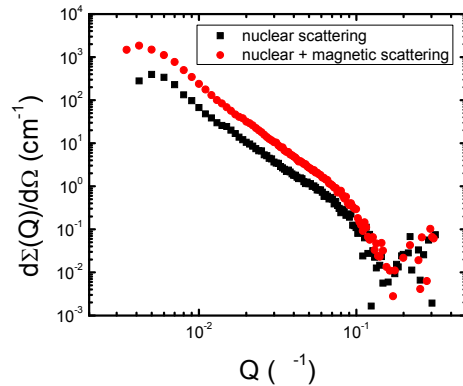
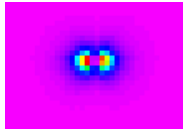
- Estimated mean void swelling ~0.3%
- Based on a measured cavity number density of $2.5 \times 10^{20} \text{ m}^{-3}$.

155 dpa, 440°C zone: EFTEM images

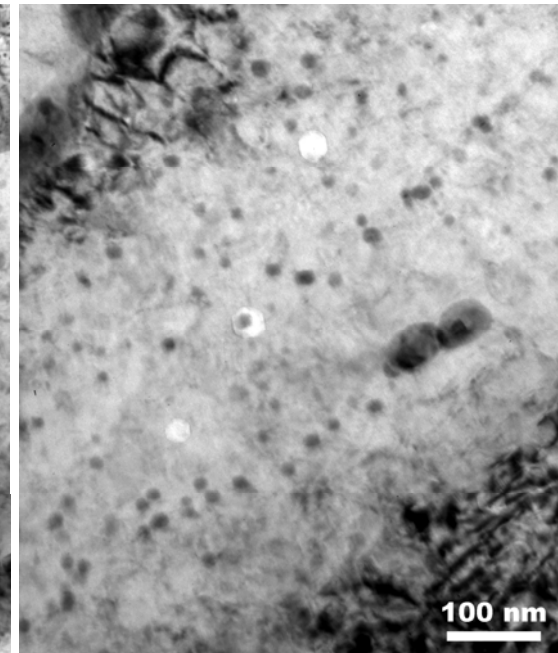
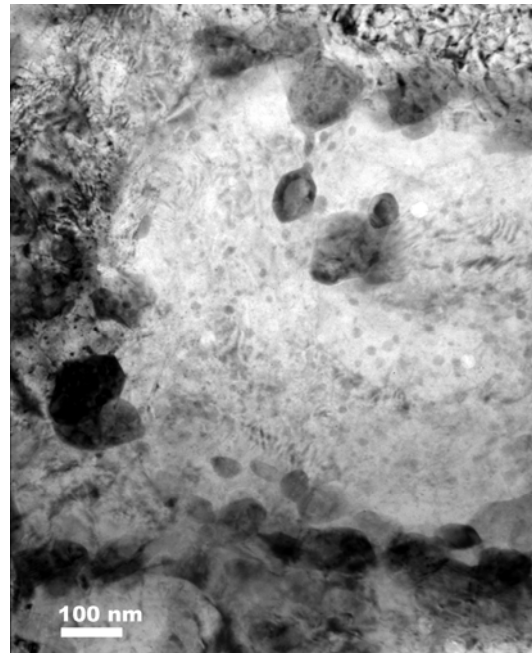
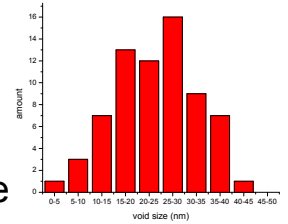


- Mn, Ni, and Si jump ratios
- Particles at the boundaries are Cr rich carbides ($M_{23}C_6$)
- Loops are not seen in any of the EFTEM images.

100 dpa, 410° C zone



- Average void size 23 nm;
- Not yet in steady state swelling regime;
- G-phase abundantly present inside grains;
- A-ratio indicates dominant carbide presence or additive contribution of several particle types (most likely)



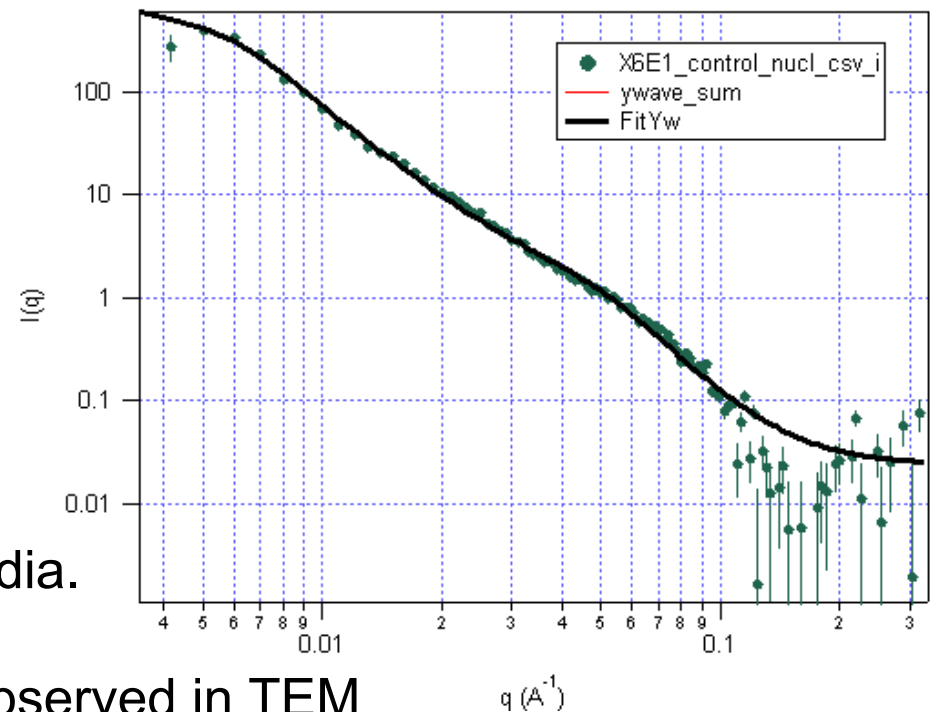
UNCLASSIFIED

Slide 25

100 dpa, 410° C zone

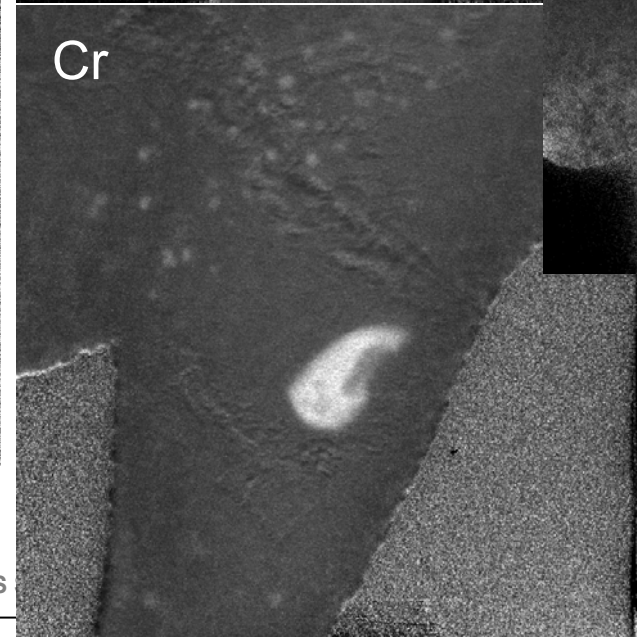
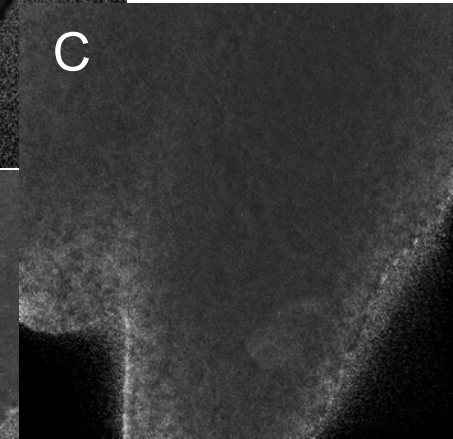
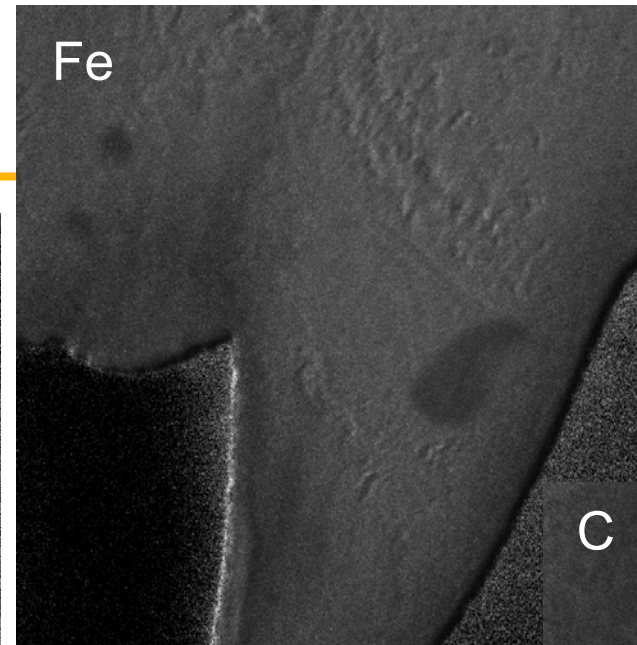
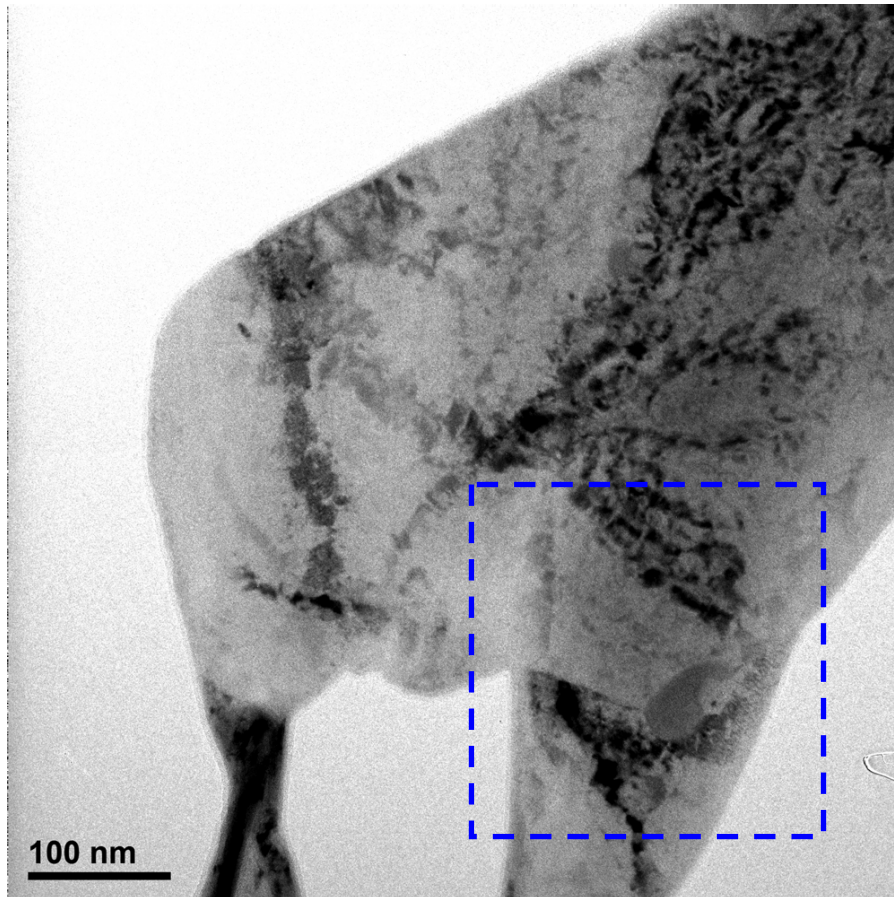
Guinier-Porod fit of both nuclear scattering and magnetic scattering indicates:

- Bimodal particle distribution
- Small smooth hard spheres
- Larger irregular spheroid particles
- Large particles of ~ 74 nm dia.
- Small particles/defects of ~ 10 nm dia.

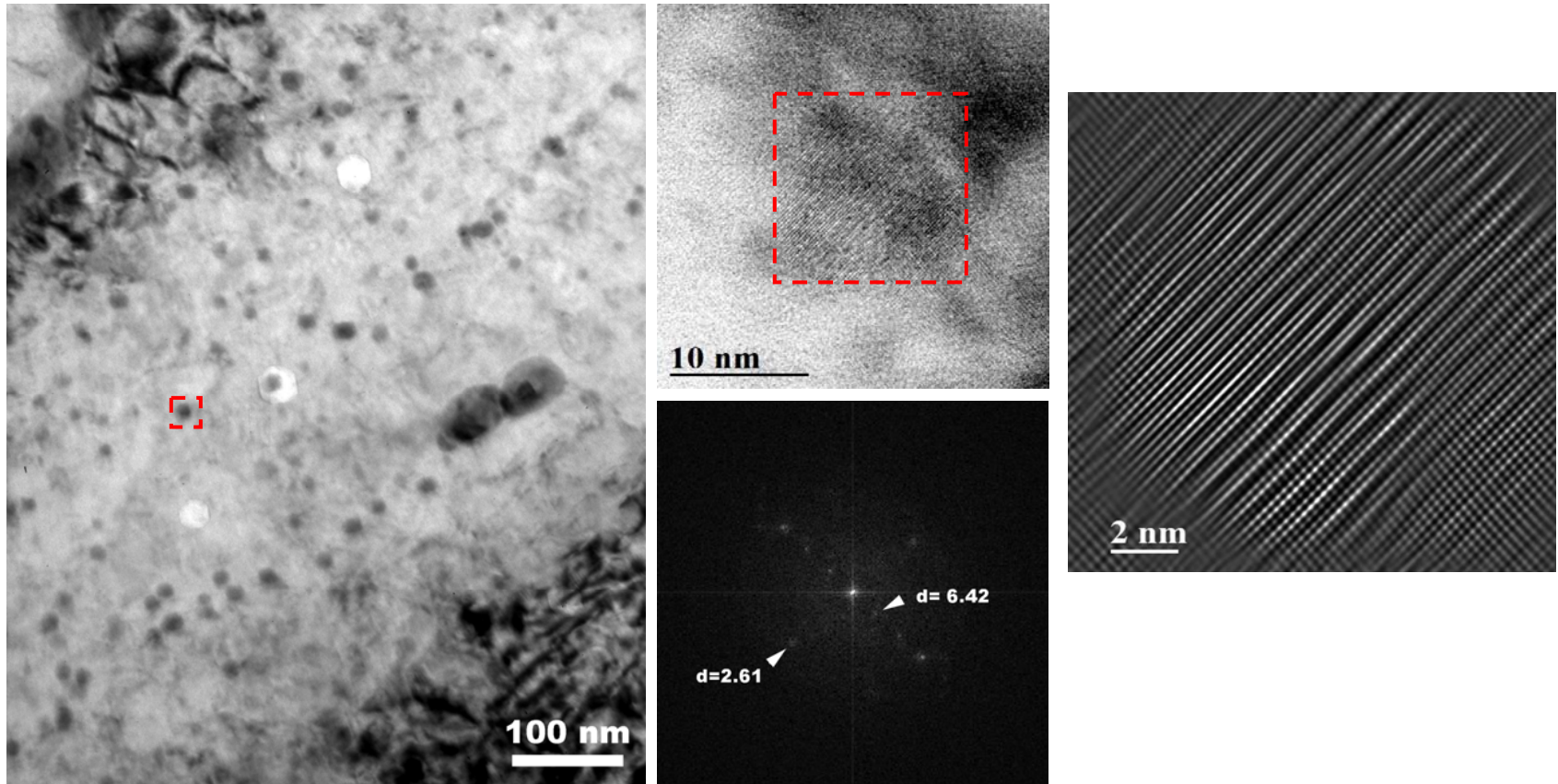


Corresponding to G-phase sizes observed in TEM

100 dpa, 410° C zone: EFTEM images



100 dpa, 410° C zone: G-phase

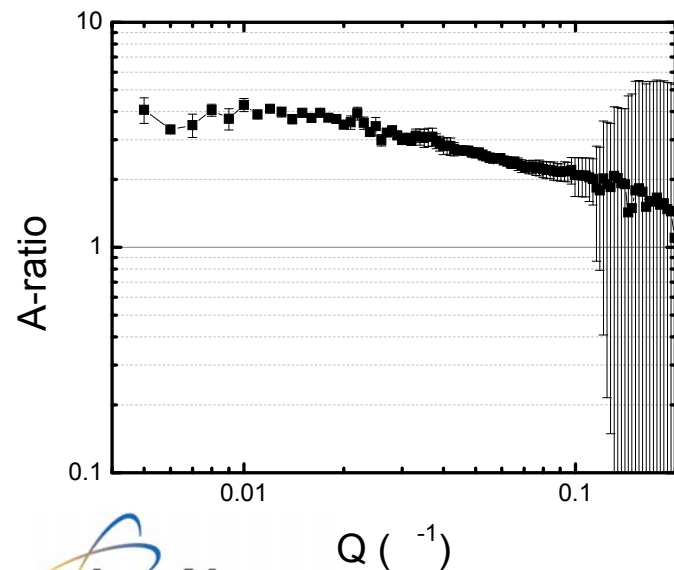
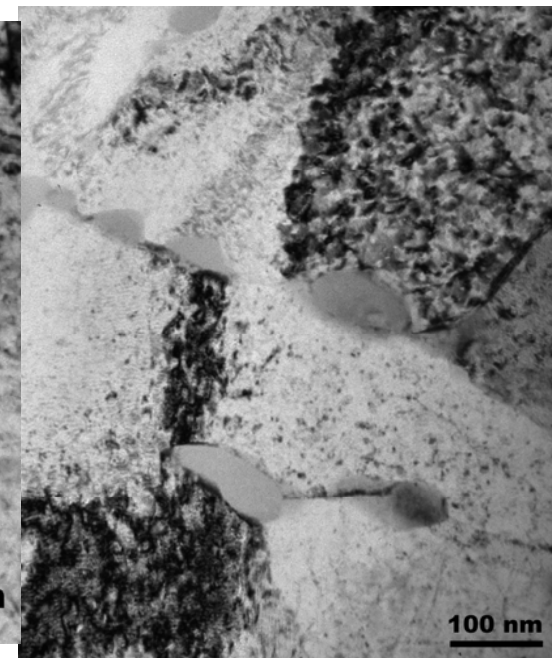
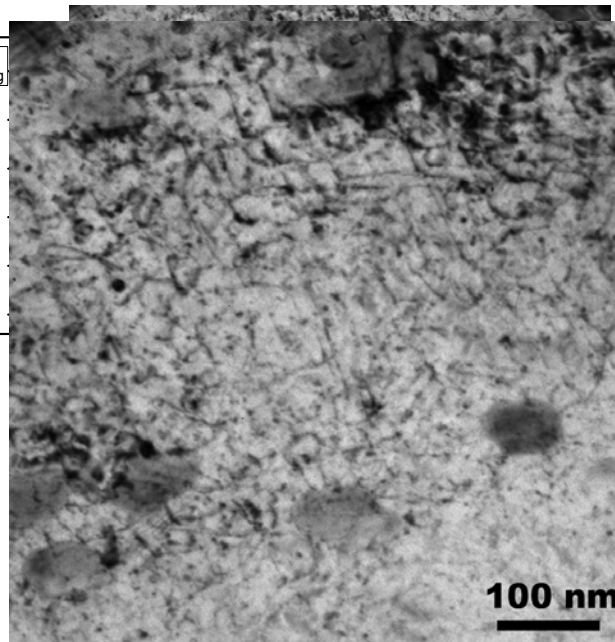
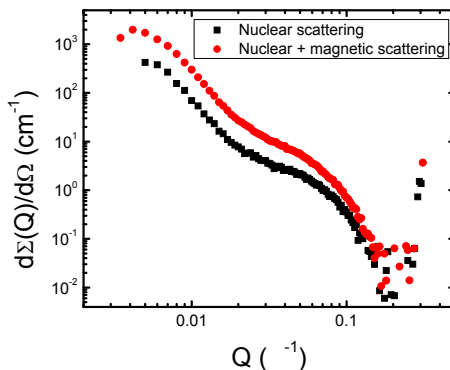
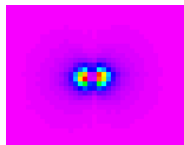


G-phase ($\text{Mn}_6\text{Ni}_{16}\text{Si}_7$): $d_{111} = 6.45 \text{ \AA}$; $d_{331} = 2.56 \text{ \AA}$

Ref. Yan *et al.*, JAC (2009) 152-155.

UNCLASSIFIED

20 dpa, 380° C zone



- $M_{23}C_6$ decorating grain and lath boundaries;
- High density of dislocation pinning particles or defects;
- A-ratio indicating dominant presence of carbides at low Q;
- Scattering curve shows significant increase of scattering in the 1-5 nm size range (to be identified by TEM)

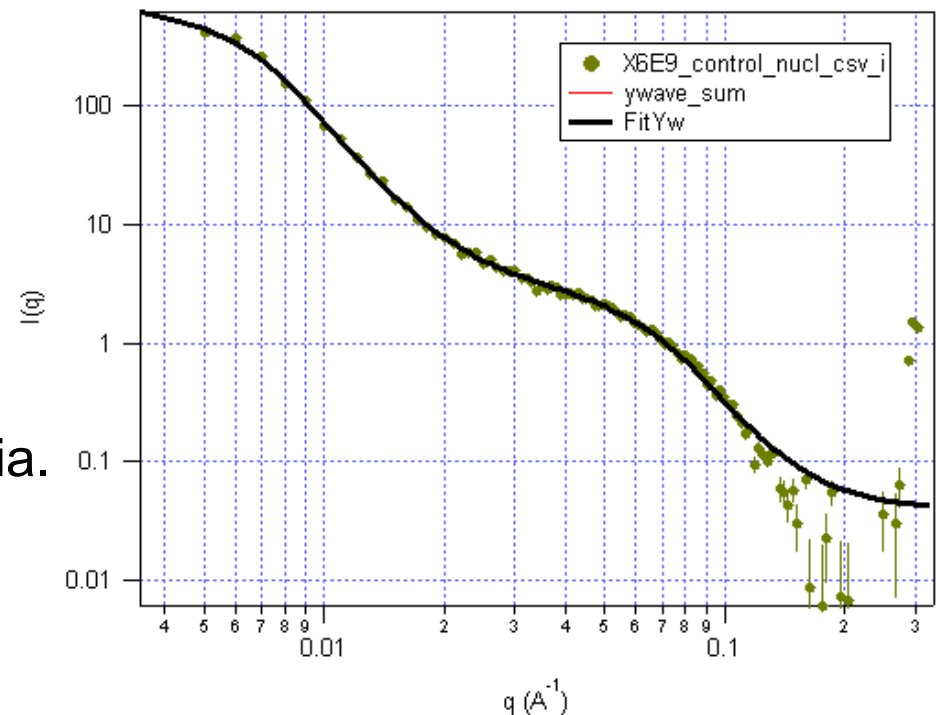
UNCLASSIFIED

Slide 29

20 dpa, 380° C zone

Guinier-Porod fit of both nuclear scattering and magnetic scattering indicates:

- Bimodal particle distribution
- Smooth hard spheres
- Large particles of ~ 72 nm dia.
- Small particles/defects of ~ 7 nm dia.



Outline

- **Introduction**
 - Background
 - Objective
 - ACO-3 duct
- **SANS & TEM analysis of the ACO-3 duct**
 - SANS measurements at LANL's Lujan Center
 - SANS and TEM results
- **Summary**

Summary and Conclusions

- A duct of HT9 irradiated up to 155 dpa over a period of 6 years in FFTF was analysed by SANS and TEM;
- The high temperature, low dpa zone (505° C, 2 dpa) showed no alterations of microstructure or presence of irradiation defects. SANS indicates probable carbide coarsening;
- High dpa, medium temperature zone (410-440° C, 100-155 dpa) reveal presence of G-phase and voids (not yet steady state swelling regime). SANS indicates dominant presence of Cr-rich precipitates;
- Low temperature, intermediate dpa zone (380° C, 20 dpa) shows high density of dislocation pinning particles or irradiation defects. SANS indicates a large increase in scattering in the 5-7 nm size range;
- Detailed TEM (HR-TEM, STEM, EFTEM) is ongoing to fully characterize microstructure and support better understanding of SANS results.